Title
Weight functions for a finite width plate with single or double radial cracks at a circular hole

Authors
Kim, Jihwi
Hill, Michael R

Publication Date
2016-12-01

DOI
10.1016/j.engfracmech.2016.10.002

Peer reviewed

Weight functions for a finite width plate with single or double radial cracks at a circular hole

Jihwi Kim and Michael R. Hill[1]
Department of Mechanical and Aerospace Engineering, University of California, Davis
One Shields Avenue, Davis, CA 95616, United States

To appear in Engineering Fracture Mechanics
Accepted October 2016
http://dx.doi.org/10.1016/j.engfracmech.2016.10.002

ABSTRACT

This work develops accurate weight functions for a single crack at a hole in a finite width plate for various hole sizes. In order to develop an accurate weight function, we first obtain accurate stress intensity factors, using the finite element method (FEM), for a reference load case of uniform stress on the crack line. Following the earlier approach for developing a weight function suggested by Wu and Carlsson, we fit the reference stress intensity factor data from FEM to a smooth analytic function; however, for the open hole it is necessary to adopt a piecewise polynomial to fit the stress intensity factor data, in place of the single polynomial suggested by Wu and Carlsson. We validate the new weight function for the case of remote uniform applied stress, which induces a stress field on the crack line exhibiting the well-known stress concentration at the hole, and for which we have accepted stress intensity factor solutions. The new weight functions provide stress intensity factors that agree very well with results from two commercial fracture mechanics software packages. Comparing results from the new and earlier weight functions shows good agreement for some crack line stress fields, but errors of a few percent for other stress fields, with the new weight function providing more reasonable results. The improved quality of the new weight functions is due both to the new reference solution for uniform crack line stress and to the piecewise fit to the reference stress intensity data. Trivial changes to the FEM model allow us to provide additional weight functions for the cases of symmetric double cracks at a hole (by adding a symmetry plane to the FEM mesh) and a single crack at a hole in a square plate (by reducing the length of the FEM mesh).

KEYWORDS

Weight function, Radial crack, Open hole, Stress intensity factor, Fracture mechanics

1. INTRODUCTION

Wu and Carlsson developed a library of weight functions for cracks in many different geometries [1]. Generally, these have good accuracy, but their weight function for a single crack at a hole in a long, finite width strip (Figure 1) was found to have limited accuracy in recent work [2]. One inaccuracy arises because their solutions are for a limited range of geometry, and

[1] Corresponding author, mrhill@ucdavis.edu, +1-530-754-6178

our earlier work used test coupons that fell outside of that range. But, there are additional causes of inaccuracy, as will be made clear below. Therefore, the goal in the present work is to develop a more accurate weight function for a crack at a hole in a finite width plate.

Weight functions are derived from a known reference load case (1), for which the stress intensity factor and crack face displacement are known [3,4]. The definition of the weight function is

$$m(a,x) = \frac{E'}{K^{(1)}(a)} \frac{\partial u^{(1)}(a,x)}{\partial a}, \tag{1}$$

where a is the crack size, x is the coordinate along the cracking-driving direction, with origin at the crack mouth, E' is the effective elastic modulus (E for plane stress and $E/(1-\nu)$ for plane strain), and $u^{(1)}(a,x)$ is the vertical (opening) displacement of the crack face under loading system (1). Given the weight function, the stress intensity factor $K^{(2)}(a)$ of any load system (2) may be found from the weight function $m(a,x)$ and the crack-line stress in the uncracked body due to load system (2), $\sigma^{(2)}(x)$. The specific expression for $K^{(2)}(a)$ is

$$K^{(2)}(a) = \int_0^a \sigma^{(2)}(x) \cdot m(a,x) dx \,. \tag{2}$$

Petroski and Achenbach [5] and Wu [6] showed that the crack face displacement of a center or edge crack can also be expressed as a function of the reference stress intensity factor, so the reference stress intensity factor is the only unknown and is the key factor related to the accuracy of a specific weight function. In addition, according to Wu and Carlsson [1], uniform stress on the crack-line is the best choice for the reference load case, because of its mathematical simplicity.

However, for cracks at a hole in a long strip [1], the only available reference solution is for remote uniform stress, for which accurate stress intensity factors are available [7]. In this case, the crack-line stress field is non-uniform, owing to the stress concentration at the hole. This allowed us to improve upon the earlier work of Wu and Carlsson. First, we developed a reference solution using uniform crack-line stress for a crack at a hole in a finite width strip. Second, piecewise polynomials were used to fit the reference stress intensity factor data, instead of using a single power series polynomial, as Wu had proposed [6]. This second step was required because the stress intensity factor solution for a crack at a hole has a rather complicated shape, with high gradients and curvature for both short and long cracks.

Following the same procedure as for a single crack in a long strip with an open hole, two additional weight functions were developed: (i) double-sided cracks in a long strip with an open hole, and (ii) a single crack in a square plate with an open hole. The square plate may provide a first approximation of the weight function for a cracked lug. For the double-sided cracks at a hole, it is assumed that the both radial cracks have the same length, and the stress distribution on the crack-line is symmetric with respect to the vertical center line.

2. METHODS

2.1. Geometries of Interest

Here, a weight function for a single crack in a long strip with an open hole (Figure 1) is developed. The weight function varies depending on the ratio of the half width of the strip (B) to the hole radius (R), so six different geometries, B/R = 2, 2.5, 3, 4, 6, 6.27 and 10, are considered (where B/R = 2 represents a large hole and B/R = 10 represents a small hole, relative to the strip width).

2.2. Wu and Carlsson's Weight Function for a Long Strip with a Circular Hole

For any B/R, Wu and Carlsson [1] expressed the reference stress intensity factor in a normalized form, called the reference geometry factor

$$f_r(a/W) = \frac{K_r(a/W)}{\sigma\sqrt{\pi a}} \tag{3}$$

which they fitted using a power series with crack size

$$f_r(a/W) = \sum_{i=0}^{I} \alpha_i \left(\frac{a}{W}\right)^i \tag{4}$$

where

K_r: reference stress intensity factor
a: crack size
σ: normalizing stress magnitude
W: ligament width (see Figure 1)
α_i: polynomial coefficients for the reference geometry factor (i = 0, 1, 2, …, I)
I: order of polynomial for the reference geometry factor.

The crack-line stress that produces the reference stress intensity factor was also expressed as a power series

$$\frac{\sigma_r(x/W)}{\sigma} = \sum_{m=0}^{M} S_m \left(\frac{x}{W}\right)^m \tag{5}$$

where

x: coordinate along the crack-line starting from the edge of a circular hole
σ_r: reference crack-line stress
S_m: polynomial coefficients of the crack-line stress (m = 0, 1, 2, …, M)
M: order of polynomial for the reference crack-line stress.

An approximate weight function can be derived [1] from the reference stress intensity solution and stress field, and for an edge crack is

$$m(a,x) = \frac{1}{\sqrt{2\pi a}} \sum_{i=1}^{3} \beta_i(a/W) \cdot \left(1 - \frac{x}{a}\right)^{i-\frac{3}{2}} \tag{6}$$

where

$$\beta_1(a/W) = 2.0$$
$$\beta_2(a/W) = \frac{1}{f_r(a/W)}\left[\frac{4a}{W}f_r'(a/W) + 2f_r(a/W) + \frac{3}{2}F_2(a/W)\right] \tag{7}$$
$$\beta_3(a/W) = \frac{1}{f_r(a/W)}\left[\frac{a}{W}F_2'(a/W) - \frac{1}{2}F_2(a/W)\right]$$

and

$$F_1(a/W) = 4f_r(a/W)$$
$$F_2(a/W) = \frac{1}{E_2(a/W)}\left[\sqrt{2}\pi\phi(a/W) - E_1(a/W)\cdot F_1(a/W)\right] \tag{8}$$

with

$$\phi(a/W) = \frac{1}{(a/W)^2}\int_0^{a/W} s\cdot[f_r(s)]^2 ds \tag{9}$$

$$\phi'(a/W) = -\frac{2}{a/W}\phi(a/W) + \frac{1}{a/W}[f_r(a/W)]^2 \tag{10}$$

$$E_j(a/W) = \sum_{m=0}^{M}\frac{2^{m+1}m!\,S_m(a/W)^m}{\prod_{k=0}^{m}(1+2j+2k)}. \tag{11}$$

The weight function of Eq. (6) has dimensionality that is consistent with Eq. (1) (one over square root of length). Wu and Carlsson [1] pursue a dimensionless analysis, and provide a similar equation for $m(a,x)$ that is non-dimensional, equal to Eq. (6) multiplied by $W^{1/2}$.

2.3. Calculation of Reference Stress Intensity Factors

In order to obtain the reference stress intensity factor under uniform stress for each geometric configuration (i.e., value of B/R), a two-dimensional FEM model was constructed with a plane stress formulation and elastic material properties $E/\sigma = 1000$ (where σ is a normalizing stress magnitude) and $\nu = 0.33$. For convenience, a half-symmetric body was analyzed, with symmetry about the crack-line, $y = 0$. The mesh was constructed with an increasing level of refinement toward the crack-line and the hole, and was composed of four-node bilinear plane stress quadrilateral elements (Figure 2). Unit uniform stress was applied on the crack face. From the finite element analysis, the *J*-integral was found for a range of crack size (14 points between a/W = 0 and 0.1, 5 points per 0.1 between 0.1 and 0.3, and 4 points per 0.1 between 0.3 and 0.9, for a total of 48 points). The reference stress intensity factor for each crack size was calculated from

$$K_r(a/W) = \sqrt{J(a/W) \cdot E} \tag{12}$$

and then the reference geometry factor, $f_r(a/W)$, was computed using Eq. (3).

Mesh refinement was carefully studied to ensure accurate reference geometry factors. Initial geometry factors were developed using a refined mesh having: 400 elements of uniform size (along x) on lines (1) and (4) of Figure 2 (the crack plane and symmetry plane, respectively); 200 elements biased along line (2) so that node spacing was smaller at the symmetry plane and twice as large at the upper end of line (2); 200 elements along line (3), biased so node spacing at the upper edge of the mesh was twice as large as at the bottom of line (3). More refined meshes were developed by halving node spacing (each quadrilateral element divided into 4 elements) and the analysis rerun until stress intensity factors converged to better than 0.1%. Accurate stress intensity factors were found with meshes having 3200 elements along lines (1) and (4) for the shortest cracks, and having 800 elements along these lines for longer cracks.

2.4. Fitting the Reference Geometry Factor with Piecewise Spline Curves

To fit accurately the reference geometry factor data from FEM, piecewise polynomial splines were used, because they can approximate a function over a large interval with smaller error than can the single polynomial used in the prior work (i.e., Eq. (4)). Piecewise polynomial splines also have global smoothness, even at breakpoints, which are endpoints of each piecewise interval. To have smooth derivatives of the polynomial splines, geometry factor data were fit with fifth order B-splines, which can be written [8] as a recurrence relation

$$f_r(a/W) = \sum_{j=1}^{m} c_j B_{j,d=5}(a/W), \tag{13}$$

where

$$B_{j,d}(a/W) = \frac{a/W - t_j}{t_{j+d} - t_j} B_{j,d-1}(a/W) + \frac{t_{j+1+d} - a/W}{t_{j+1+d} - t_{j+1}} B_{j+1,d-1}(a/W) \tag{14}$$

and

$$B_{j,0}(a/W) = \begin{cases} 1, & if\ t_j \leq a/W < t_{j+1} \\ 0, & otherwise. \end{cases} \tag{15}$$

with

a: crack size
$f_r(a/W)$: spline fit for the reference geometry factor
d: order of a spline, taken as 5
$B_{j,d}$: j^{th} B-spline of d^{th} order
c_j: coefficients of B-splines
m: number of B-splines
t_j: knots, non-decreasing sequence of real numbers, $j = 1, 2, \ldots, m + d + 1$.

The knot sequence t_j includes breakpoints for the splines, including the two global endpoints (the first and last points of the knot sequence) each occurring d+1 times, so that the spline passes through the endpoints. Trial and error was used to find a useful number of piecewise polynomial intervals, and the trials provided $m = 7$ intervals between global endpoints of $a/W = 0$ and 0.9, with six break points between. For all but one geometry, the breakpoints, found by trial and error, are 0.05, 0.15, 0.25, 0.45, 0.65, and 0.8; for B/R = 10, the breakpoints are 0.03, 0.08, 0.15, 0.35, 0.55 and 0.7. Therefore, the knot sequence vectors for the splines are {0, 0, 0, 0, 0, 0, 0.05, 0.15, 0.25, 0.45, 0.65, 0.8, 0.9, 0.9, 0.9, 0.9, 0.9, 0.9} for all but B/R = 10, and {0, 0, 0, 0, 0, 0, 0.03, 0.08, 0.15, 0.35, 0.55, 0.7, 0.9, 0.9, 0.9, 0.9, 0.9, 0.9} for B/R = 10. The coefficients of B-splines, c_j were calculated from the 48 reference geometry factor values from FEM using least squares. For convenience, the B-spline reference geometry factor fit of Eq. (13) will be written with a polynomial form, so the coefficients α_i of Eq. (4) will be reported for each piecewise interval.

2.5. Computing $\beta_i(a/W)$ Function Values

The weight function is a linear combination of $\beta_i(a/W)$ functions, each multiplied by a function of x/a, and $\beta_i(a/W)$ functions are determined from reference geometry factor piecewise spline fits ($f_r(a/W)$) and crack-line stress related terms ($E_j(a/W)$). Because the loading is a simple unit uniform stress on the crack-line, $E_i(a/W)$ in Eq. (11) become constants, which are

$$E_1(a/W) = \frac{2}{3} \; and \; E_2(a/W) = \frac{2}{5}, \tag{16}$$

and the determination of $\beta_i(a/W)$ is dramatically simplified. Substituting Eq. (8) and (16) into Eq. (7),

$$\begin{aligned} \beta_1(a/W) &= 2.0 \\ \beta_2(a/W) &= \frac{1}{f_r(a/W)}\left[\frac{4a}{W} f_r'(a/W) - 8 f_r(a/W) + \frac{15\sqrt{2}\pi}{4}\phi(a/W)\right] \\ \beta_3(a/W) &= \frac{1}{f_r(a/W)}\left[\frac{5\sqrt{2}\pi a}{2W}\phi'(a/W) - \frac{5\sqrt{2}\pi}{4}\phi(a/W) \right. \\ &\quad \left. - \frac{20a}{3W} f_r'(a/W) + \frac{10}{3} f_r(a/W)\right]. \end{aligned} \tag{17}$$

In Eq. (17), $f_r'(a/W)$ is obtained by derivation of a piecewise polynomial form of $f_r(a/W)$ in Eq. (13). The function $\phi(a/W)$ and its derivative $\phi'(a/W)$ (Eq. (9) and (10) respectively) include the integration of a polynomial of eleventh order, so sixth order Gaussian quadrature was used for the accurate numerical integration (n-th order Gaussian quadrature is accurate for all polynomials up to order $2n-1$).

2.6. Computing Geometry Factor

Once a weight function is known, a new geometry factor due to a given arbitrary crack-line stress can be calculated using Eq. (2) and Eq. (3) and written with Eq. (6) as

$$f(a/W) = \frac{1}{\sqrt{2\pi a}} \int_0^a \frac{\sigma(x)}{\sigma} \sum_{i=1}^{3} \beta_i(a/W) \left(1 - \frac{x}{a}\right)^{i-\frac{3}{2}} dx \tag{18}$$

where $\sigma(x)$ is an arbitrary crack-line stress field. To compare the present work to the earlier work of Wu and Carlsson, we determine $f(a/W)$ for two stress fields, one being the crack-line stress due to remote loading and the other being uniform crack-line stress. For remote loading, the crack-line stress $\sigma(x)$ is required, and was found from the same finite element meshes used to determine the stress intensity factors, but the model contained no crack, and uniform stress was applied on the remote boundary (i.e., at the top and bottom edge of Figure 1).

2.7. Additional Weight Functions

The FEM models described above were altered to develop weight functions for two other geometries, one geometry being two symmetric cracks at a hole in a long strip, and the other being a single crack at a hole in a square plate. For symmetric cracks, a vertical symmetry plane was introduced along the line (5) in Figure 2, all nodes and elements to the left of that line were removed, and the analyses repeated to develop new stress intensity factors. For the square plate, all nodes and elements were removed from the upper region of the strip model (areas near line (3) in Figure 2), and the analyses were repeated. From the modified FEM model results, reference geometry factors are obtained and fitted with piecewise spline curves, then $\beta_i(a/W)$ functions in Eq. (18) are calculated. Geometry factors are also calculated to verify the weight functions.

3. RESULTS

3.1. Reference Geometry Factors

Reference geometry factors for a single crack at a hole under uniform crack-line stress are expressed as 5th-order piecewise polynomials, with the six coefficients for each geometry given in Table 1. The reference geometry factor for B/R = 2 is shown in Figure 3(a). The seven, 5th-order piecewise polynomials fit the FEM results with a high degree of accuracy (around 0.02% maximum difference). Figure 3(b) shows the derivative of the piecewise polynomial fit, which is smooth over the whole range, including the breakpoints. Figure 4(a) shows the two piecewise polynomials for $0 < a/W < 0.05$ and $0.05 < a/W < 0.15$, which fit the FEM results very well in their intervals. A 7th-order single polynomial was fit for the whole range ($0 < a/W < 0.9$), and is shown for comparison, having a maximum misfit of 0.11%. Figure 4(b) shows that the single polynomial curve expresses the FEM results less accurately near the concave region ($a/W = 0.15$).

3.2. $\beta_i(a/W)$ Values

The calculated $\beta_i(a/W)$ values for a single crack at a hole are given for selected crack sizes in Table 2. A more complete table of $\beta_i(a/W)$ values is provided as an attachment. For selected geometries (B/R = 2, 4, and 6), the newly calculated $\beta_i(a/W)$ values are plotted and compared to those from Wu and Carlsson (W&C) (B/R = 2, 3.5, and 5) in Figure 5. In Figure 5(a), there is good agreement for B/R = 2, but for other B/R, $\beta_2(a/W)$ is smooth for the present results, but wavy for the earlier work. In Figure 5(b), $\beta_3(a/W)$ from this work for B/R = 2, 4, and 6 have a similar form, but $\beta_3(a/W)$ for the earlier work is again wavy. The waviness observed in $\beta_2(a/W)$ and $\beta_3(a/W)$ is discussed below.

3.3. Stress Intensity Factor Solutions for Point Loads (Green's Function)

The geometry factor for opposing point loads applied on the crack face is known as the Green's function, and is expressed as

$$G(a/W\,, x/a) = \frac{\sqrt{2}}{2}\left\{2\left(1-\frac{x}{a}\right)^{-\frac{1}{2}} + \beta_2(a/W)\cdot\left(1-\frac{x}{a}\right)^{\frac{1}{2}} \right. \\ \left. + \beta_3(a/W)\cdot\left(1-\frac{x}{a}\right)^{\frac{3}{2}}\right\}. \tag{19}$$

Figure 6 shows Green's function for B/R = 2. Figure 6 has four sub-figures that include (a) Green's function for x/a = 0, 0.5, 0.8, and 0.9, (b) same as (a) but focused on $0 < a/W < 0.4$, (c) Green's function for x/a = 0, 0.1, 0.2, 0.3, and 0.5, and (d) same as (c) but focused on $0 < a/W < 0.4$. At $x = 0$, the Green's function from this work agrees with Wu and Carlsson with difference less than 2% except in the range of $0.01 < a/W < 0.23$ where the maximum difference increases up to 6%. As the position of the point load (x/a) increases, the differences decrease.

The Green's function for point loads at specific locations are compared in Figure 7 for a range of B/R. Figure 7(a) shows the Green's function for point loads at $x/a = 0$ and Figure 7(b) is focused for smaller crack sizes, $0 < a/W < 0.4$. Figure 7(c) and (d) show similar Green's function results for point loads at x/a = 0.5 and 0.9, respectively. The Green's function values decrease as B/R increases. While the results of this work are smooth and self-similar, results from the earlier work become wavier as B/R increases.

3.4. Geometry Factors

Geometry factors for unit uniform crack-line pressure ($\sigma(x) = 1$) are shown in Figure 8(a) and (b). Discrepancies among the current weight function method (this work), the earlier work (W&C), and the commercial package (NASSIF, TC13 [9]) are apparent for small crack sizes ($a/W < 0.2$). There is reasonable agreement for larger crack sizes between this work and the earlier work, but the discrepancies continue between this work and the NASSIF results after a/W = 0.2 for some geometries. Some waviness is apparent in results based on the earlier work and the NASSIF results, but the new results are smooth.

For remote load, crack-line stresses are concentrated at the hole, as shown in Figure 9(a). Geometry factors calculated with the current weight function method (this work), the earlier work, and commercial packages (AFGROW [10] and NASSIF, TC13 [9]) are shown in Figure 9(b). In addition, the theoretical value of the geometry factor at $a/W = 0$ is shown, estimated as 1.12 times the stress concentration factor at the hole, (SCF), the SCF being taken from [11]. There is good agreement among all the results for B/R = 2 and 2.5, and the results for the other geometry cases (B/R = 3, 4, 6, and 10 for this work and B/R = 3.5 and 5 for the earlier weight function) are reasonably placed in the order of the B/R ratio. Results of the present weight function also fall between those from the commercial packages.

3.5. Additional Weight Functions

Coefficients of the piecewise polynomials of the reference geometry factor are provided in Table 3 and Table 4 respectively. In addition, $\beta_i(a)$ values for these additional cases are listed in Table 5 and Table 6, respectively. Comparison plots of geometry factors due to uniform crack-line pressure and remote load for double-sided cracks in a long strip with an open hole are shown in Figure 10 and Figure 11. While the crack-line pressure case shows obvious discrepancies with commercial software, the remote load case shows excellent agreement with them.

4. DISCUSSION

4.1. Reasons of Waviness of $\beta_i(a/W)$ and $G(a/W, x/a)$

The waviness of $\beta_2(a/W)$ from Wu and Carlsson is caused by the derivative of the reference geometry factor that is a high order single polynomial. From Eq. (17), we have

$$\beta_2(a/W) = 4g_1(a/W) - 8 + \frac{15\sqrt{2}\pi}{4} g_2(a/W) \tag{20}$$

where

$$\begin{aligned} g_1(a/W) &= \frac{\frac{a}{W} f_r'(a/W)}{f_r(a/W)} \\ g_2(a/W) &= \frac{\phi(a/W)}{f_r(a/W)}. \end{aligned} \tag{21}$$

Figure 12(a) and (b) compare $f_r(a/W)$ and $f_r'(a/W)$ for this work and the W&C work, for a mid-value of B/R. Figure 12(c) compares $g_1(a/W)$, which is a dominant term in Eq. (20). The $g_1(a/W)$ of W&C is wavy and similar to $\beta_2(a/W)$ (Figure 12(d)) while $g_1(a/W)$ for this work is smooth. The waviness of $g_1(a/W)$ seems to be due to the waviness of $f_r'(a/W)$. $\beta_3(a/W)$ is more complex than $\beta_2(a/W)$, but the dominant term in the waviness is also $f_r'(a/W)$.

4.2. Geometry Factors

Geometry factors for the earlier work show inconsistent curve shapes between the different B/R, with waviness consistent with waviness of the Green's function, while the geometry factors for this work have an improved shape. These characteristics are shown more clearly by plotting a ratio of geometry factor for various B/R to the geometry factor for B/R = 2 of this work. In the plot of geometry factor ratio for uniform crack-line stress (Figure 13(a) and (b)), the curves for this work are smooth and self-similar, but the curves for the earlier work show the waviness noted earlier. However, the geometry factor ratios for remote load (Figure 13(c) and (d)) are very close to one another, and show less waviness. From these comparisons, it seems that the earlier weight function may have different quality, depending on the applied load, while results for this work show consistent quality regardless of loading.

5. CONCLUSIONS

This work developed accurate weight functions for a radial crack at a hole in a strip for B/R = 2, 2.5, 3, 4, 6, 6.27, and 10. The present work first focused on finding accurate reference stress intensity factors because they are a key factor for developing an accurate weight function. Uniform crack-line stress was used as the load case for the reference stress intensity factor, and 5th-order piecewise polynomial splines were used to fit the reference stress intensity factors found from finite element analysis. With an accurate approximation for the new reference stress intensity factor, we developed parameters for the new weight function. The new weight function provides stress intensity factors due to the point loads and uniform crack-line stress that are smooth and self-similar, unlike results from an earlier weight function. The new weight function also provides stress intensity factors for remote loads that agree well with those from typical commercial software packages.

REFERENCES

[1] Wu, X. R. and Carlsson, J., Weight functions and stress intensity factor solutions, Pergamon, 1991.

[2] Stuart, D. H., Hill, M. R., and Newman Jr., J. C., "Correlation of one-dimensional fatigue crack growth at cold-expanded holes using linear fracture mechanics and superposition," Engineering Fracture Mechanics, vol. 78, no. 7, pp. 1389–1406, May 2011.

[3] Bueckner, H. F., "A novel principle for the computation of stress intensity factors," Z. Angew. Math. Mech., vol. 50, pp. 529–546, 1970.

[4] Rice, J. R., "Some remarks on elastic crack-tip stress fields," International Journal of Solids and Structures, vol. 8, no. 6, pp. 751–758, 1972.

[5] Petroski, H. J. and Achenbach, J. D., "Computation of the weight function from a stress intensity factor," Engineering Fracture Mechanics, vol. 10, no. 2, pp. 257–266, 1978.

[6] Wu, X. R., "Approximate weight functions for center and edge cracks in finite bodies," Engineering Fracture Mechanics, vol. 20, no. 1, pp. 35–49, 1984.

[7] Newman Jr, J. C., "An improved method of collocation for the stress analysis of cracked plates with various shaped boundaries," NASA TN D-6376, August 1971.

[8] Schumaker , L. L., Spline Functions: Basic Theory, 3rd ed. Cambridge University Press, 2007.

[9] NASGRO version 6.21. NASA Johnson Space Center and Southwest Research Institute; 2012.

[10] Harter, J., AFGROW User's Guide and Technical Manual, AFGROW version 4.0012.15. AFRL-VA-WP-TR-2008. 4.0012.15 ed. Wright-Patterson Air Force Base, Ohio 2008.

[11] Pilkey, W. D. and Pilkey, D. F., Peterson's Stress Concentration Factors, 3rd ed. John Wiley, Chart 4.1, pp. 270, 2008.

TABLES

Single crack (Long strip with a hole, H/B ≥ 2)								
B/R	**Polynomial**	**Interval**	α_0	α_1	α_2	α_3	α_4	α_5
2	1	0 < a/W < 0.05	1.1200125	-0.80763166	7.9355633	-100.81862	994.09834	-4055.5336
	2	0.05 < a/W < 0.15	1.1187217	-0.67855268	2.7724042	2.4445643	-38.533495	74.993714
	3	0.15 < a/W < 0.25	1.1269285	-0.95211242	6.4198673	-21.871857	42.521242	-33.079269
	4	0.25 < a/W < 0.45	1.0933887	-0.28131771	1.0535096	-0.40642595	-0.40961970	1.2654203
	5	0.45 < a/W < 0.65	0.95083523	1.3026101	-5.9861697	15.237306	-17.791544	8.9907200
	6	0.65 < a/W < 0.80	-16.954556	139.03639	-429.78240	667.23151	-519.32554	163.30887
	7	0.80 < a/W < 0.90	-1164.0292	7308.2530	-18352.824	23071.033	-14521.702	3663.9029
2.5	1	0 < a/W < 0.05	1.1199209	-1.1721983	6.6368645	-33.181707	190.77533	-666.51998
	2	0.05 < a/W < 0.15	1.1197181	-1.1519171	5.8256183	-16.956782	28.526078	-17.522981
	3	0.15 < a/W < 0.25	1.1204887	-1.1776031	6.1680976	-19.239978	36.136729	-27.670516
	4	0.25 < a/W < 0.45	1.0924625	-0.6170781	1.6838978	-1.3031784	0.26313048	1.0283628
	5	0.45 < a/W < 0.65	0.95932882	0.86218450	-4.8906026	13.306822	-15.970204	8.2431780
	6	0.65 < a/W < 0.80	-15.933916	130.81022	-404.73071	628.44545	-489.15376	153.83812
	7	0.80 < a/W < 0.90	-1048.5171	6584.4550	-16538.843	20796.085	-13093.929	3305.0318
3	1	0 < a/W < 0.05	1.1200326	-1.6101665	11.314142	-99.924447	827.92879	-3210.7765
	2	0.05 < a/W < 0.15	1.1190318	-1.5100920	7.3111608	-19.864826	27.332582	-8.3916980
	3	0.15 < a/W < 0.25	1.1212756	-1.5848849	8.3083994	-26.513083	49.493439	-37.939508
	4	0.25 < a/W < 0.45	1.0837252	-0.8338765	2.3003321	-2.4808142	1.4289008	0.51212285
	5	0.45 < a/W < 0.65	0.94781330	0.67625586	-4.4113673	12.434073	-15.143196	7.8774994
	6	0.65 < a/W < 0.80	-14.818988	121.95934	-377.59008	586.55518	-456.77481	143.76415
	7	0.80 < a/W < 0.90	-995.12770	6248.8888	-15694.914	19733.210	-12423.434	3135.4289
4	1	0 < a/W < 0.05	1.1201194	-2.4721241	21.961779	-216.18080	1741.6216	-6578.0708
	2	0.05 < a/W < 0.15	1.1181073	-2.2709161	13.913458	-55.214385	131.95745	-139.41414
	3	0.15 < a/W < 0.25	1.1111855	-2.0401895	10.837103	-34.705355	63.594021	-48.262896
	4	0.25 < a/W < 0.45	1.0647808	-1.1120948	3.4123457	-5.0063246	4.1959615	-0.74444760
	5	0.45 < a/W < 0.65	0.91826511	0.51585691	-3.8229953	11.072211	-13.669078	7.1955700
	6	0.65 < a/W < 0.80	-13.476201	111.24252	-344.52042	535.22209	-416.86129	131.25471
	7	0.80 < a/W < 0.90	-909.17002	5709.3289	-14339.736	18029.242	-11350.624	2864.6953
6	1	0 < a/W < 0.05	1.1201988	-4.1884339	54.782022	-663.38188	5567.3210	-21054.572
	2	0.05 < a/W < 0.15	1.1137889	-3.5474399	29.142262	-150.58668	439.36893	-542.76350
	3	0.15 < a/W < 0.25	1.0767375	-2.3123936	12.674977	-40.804785	73.429281	-54.843972
	4	0.25 < a/W < 0.45	1.0261734	-1.3011120	4.5847247	-8.4437744	8.7072594	-3.0663550
	5	0.45 < a/W < 0.65	0.83094084	0.86813907	-5.0563913	12.980928	-15.097965	7.5137449
	6	0.65 < a/W < 0.80	-11.758031	97.706383	-303.02022	471.38682	-367.71788	116.01218
	7	0.80 < a/W < 0.90	-806.50051	5064.8469	-12720.871	15993.701	-10069.164	2541.3738
6.27	1	0 < a/W < 0.05	1.1201837	-4.4000240	58.698738	-708.10978	5898.0048	-22219.016
	2	0.05 < a/W < 0.15	1.1134349	-3.7251439	31.703535	-168.20572	498.96421	-622.85352
	3	0.15 < a/W < 0.25	1.0702438	-2.2854394	12.507474	-40.231981	72.385078	-54.081349
	4	0.25 < a/W < 0.45	1.0202378	-1.2853200	4.5065193	-8.2281607	8.3774365	-2.8752361
	5	0.45 < a/W < 0.65	0.83722459	0.74816025	-4.5311705	11.855594	-13.937847	7.0426677
	6	0.65 < a/W < 0.80	-11.879041	98.565588	-305.50787	474.89667	-370.12329	116.63819
	7	0.80 < a/W < 0.90	-788.90521	4954.9792	-12446.542	15651.189	-9855.3060	2487.9339
10	1	0 < a/W < 0.03	1.1199303	-7.3122707	135.12522	-1975.6814	20782.311	-111861.34
	2	0.03 < a/W < 0.08	1.1175705	-6.9189607	108.90455	-1101.6592	6215.2744	-14747.757
	3	0.08 < a/W < 0.15	1.0719704	-4.0689547	37.654401	-211.03233	648.85643	-831.71197
	4	0.15 < a/W < 0.35	1.0108645	-2.0320928	10.496243	-29.977941	45.341811	-27.025810
	5	0.35 < a/W < 0.55	0.81957681	0.70058851	-5.1190793	14.637265	-18.394198	9.3947666
	6	0.55 < a/W < 0.70	1.2778489	-3.4655211	10.030410	-12.907262	6.6462812	0.28913797
	7	0.70 < a/W < 0.90	-55.926164	405.13457	-1157.3984	1654.8482	-1184.6076	340.64740

Table 1 – Coefficients α_i of the piecewise polynomials of the reference geometry factor for a single crack in a long strip with an open hole

a/W	$\beta_1(a/W)$	$\beta_2(a/W)$	$\beta_3(a/W)$	$\beta_1(a/W)$	$\beta_2(a/W)$	$\beta_3(a/W)$
		B/R = 2			**B/R = 2.5**	
0.01	2.00000	1.28379	0.21892	2.00000	1.25934	0.21737
0.10	2.00000	1.07432	0.18230	2.00000	0.88425	0.17222
0.20	2.00000	1.06110	0.18035	2.00000	0.74587	0.16106
0.30	2.00000	1.18123	0.16694	2.00000	0.77746	0.12617
0.40	2.00000	1.44332	0.09990	2.00000	0.97201	0.03054
0.50	2.00000	1.89209	-0.05531	2.00000	1.37288	-0.17477
0.60	2.00000	2.65011	-0.39985	2.00000	2.10896	-0.61338
0.70	2.00000	3.98797	-1.14980	2.00000	3.46072	-1.53139
0.80	2.00000	6.85984	-3.28770	2.00000	6.40013	-3.97310
0.90	2.00000	15.8901	-12.0033	2.00000	15.4942	-13.1901
		B/R = 3			**B/R = 4**	
0.01	2.00000	1.23509	0.21491	2.00000	1.18724	0.21052
0.10	2.00000	0.72617	0.16261	2.00000	0.48063	0.15886
0.20	2.00000	0.51382	0.15731	2.00000	0.19044	0.18220
0.30	2.00000	0.49615	0.12956	2.00000	0.12620	0.17791
0.40	2.00000	0.65425	0.03101	2.00000	0.24474	0.09182
0.50	2.00000	1.02695	-0.19251	2.00000	0.58419	-0.14396
0.60	2.00000	1.74474	-0.67631	2.00000	1.27819	-0.67752
0.70	2.00000	3.09525	-1.68969	2.00000	2.61829	-1.79802
0.80	2.00000	6.05087	-4.30418	2.00000	5.56963	-4.60325
0.90	2.00000	15.16420	-13.8765	2.00000	14.6301	-14.5386
		B/R = 6			**B/R = 6.27**	
0.01	2.00000	1.09730	0.20255	2.00000	1.08594	0.20170
0.10	2.00000	0.14580	0.17991	2.00000	0.11007	0.18423
0.20	2.00000	-0.20057	0.27254	2.00000	-0.24048	0.28744
0.30	2.00000	-0.29545	0.30631	2.00000	-0.33587	0.32235
0.40	2.00000	-0.20736	0.23534	2.00000	-0.24962	0.25225
0.50	2.00000	0.10805	-0.02020	2.00000	0.06316	-0.00405
0.60	2.00000	0.77573	-0.59691	2.00000	0.73043	-0.58777
0.70	2.00000	2.08896	-1.80445	2.00000	2.04088	-1.80165
0.80	2.00000	5.01246	-4.78318	2.00000	4.95580	-4.78674
0.90	2.00000	13.9260	-14.9841	2.00000	13.8517	-15.0059
		B/R = 10				
0.01	2.00000	0.93992	0.19115			
0.10	2.00000	-0.25911	0.28567			
0.20	2.00000	-0.61037	0.44032			
0.30	2.00000	-0.71897	0.50712			
0.40	2.00000	-0.62360	0.40111			
0.50	2.00000	-0.32855	0.14098			
0.60	2.00000	0.30411	-0.45087			
0.70	2.00000	1.64222	-1.80686			
0.80	2.00000	4.40498	-4.71450			
0.90	2.00000	12.5992	-14.1780			

Table 2 – $\beta_i(a/W)$ for a single crack in a long strip with an open hole for B/R = 2, 2.5, 3, 4, 6, 6.27, and 10

Double cracks (Long strip with a hole, H/B ≥ 2)								
B/R	**Polynomial**	**Interval**	α_0	α_1	α_2	α_3	α_4	α_5
2	1	0 < a/W < 0.05	1.1199803	-0.79132654	8.8128839	-87.864685	820.20325	-3330.1256
	2	0.05 < a/W < 0.15	1.1189176	-0.68505692	4.5620992	-2.8489910	-29.953691	70.502143
	3	0.15 < a/W < 0.25	1.1275595	-0.97311945	8.4029329	-28.454549	55.398170	-43.300338
	4	0.25 < a/W < 0.45	1.0833785	-0.08949973	1.3339751	-0.17871822	-1.1534923	1.9409916
	5	0.45 < a/W < 0.65	0.92589008	1.6603712	-6.4432289	17.103957	-20.356465	10.475646
	6	0.65 < a/W < 0.80	-21.182461	171.72461	-529.71780	822.14177	-639.61632	201.01714
	7	0.80 < a/W < 0.90	-1458.2202	9153.2103	-22983.432	28889.285	-18181.581	4586.5082
2.5	1	0 < a/W < 0.05	1.1199989	-1.1908629	11.358652	-96.064405	789.66491	-3071.7995
	2	0.05 < a/W < 0.15	1.1190373	-1.0946964	7.5119921	-19.131208	20.332937	5.5284363
	3	0.15 < a/W < 0.25	1.1228583	-1.2220650	9.2102398	-30.452859	58.071775	-44.790014
	4	0.25 < a/W < 0.45	1.0780051	-0.32500062	2.0337248	-1.7467987	0.65965468	1.1396824
	5	0.45 < a/W < 0.65	0.89451513	1.7137767	-7.0275078	18.389274	-21.713759	11.083422
	6	0.65 < a/W < 0.80	-21.353966	172.85594	-533.61878	828.52970	-644.89870	202.83263
	7	0.80 < a/W < 0.90	-1433.3315	8997.7153	-22595.767	28406.215	-17880.952	4511.8460
3	1	0 < a/W < 0.05	1.1200352	-1.6116083	16.415641	-146.21711	1149.2618	-4335.6366
	2	0.05 < a/W < 0.15	1.1187048	-1.4785736	11.094256	-39.789407	84.984810	-78.528597
	3	0.15 < a/W < 0.25	1.1162404	-1.3964256	9.9989498	-32.487363	60.644663	-46.075068
	4	0.25 < a/W < 0.45	1.0712325	-0.49626800	2.7976887	-3.6823191	3.0345746	0.01300297
	5	0.45 < a/W < 0.65	0.85220952	1.9373205	-8.0182602	20.353123	-23.671472	11.882357
	6	0.65 < a/W < 0.80	-21.073313	170.59518	-526.96553	818.73354	-637.81025	200.84814
	7	0.80 < a/W < 0.90	-1446.7700	9081.1994	-22803.476	28664.372	-18041.334	4551.7291
4	1	0 < a/W < 0.05	1.1200964	-2.4706654	31.473564	-339.38424	2769.1337	-10441.706
	2	0.05 < a/W < 0.15	1.1169112	-2.1521468	18.732820	-84.569354	220.98488	-249.11027
	3	0.15 < a/W < 0.25	1.1027295	-1.6794234	12.429842	-42.549503	80.918711	-62.355381
	4	0.25 < a/W < 0.45	1.0414704	-0.45424061	2.6283793	-3.3436529	2.5070109	0.37397968
	5	0.45 < a/W < 0.65	0.84197031	1.7624265	-7.2234746	18.549356	-21.818554	11.185342
	6	0.65 < a/W < 0.80	-21.977386	177.29594	-547.32658	849.47721	-660.99383	207.85466
	7	0.80 < a/W < 0.90	-1441.4270	9048.8558	-22726.226	28573.102	-17988.259	4539.6710
6	1	0 < a/W < 0.05	1.1201810	-4.1804079	74.875380	-995.41503	8573.1815	-32622.770
	2	0.05 < a/W < 0.15	1.1102289	-3.1851891	35.066630	-199.24004	611.43159	-775.77034
	3	0.15 < a/W < 0.25	1.0553288	-1.3551884	10.666621	-36.573307	69.209155	-52.807091
	4	0.25 < a/W < 0.45	1.0039286	-0.3271833	2.4425801	-3.6771449	3.4168299	-0.1732309
	5	0.45 < a/W < 0.65	0.7863487	2.0903711	-8.3021061	20.199936	-23.113260	11.617920
	6	0.65 < a/W < 0.80	-22.434741	180.71413	-557.91369	865.75621	-673.54117	211.74958
	7	0.80 < a/W < 0.90	-1394.9675	8759.0442	-22003.739	27673.038	-17428.092	4400.3873
10	1	0 < a/W < 0.03	1.1199516	-7.2502613	185.14378	-3257.0975	38685.631	-221748.31
	2	0.03 < a/W < 0.08	1.1150655	-6.4359179	130.85422	-1447.4453	8524.7616	-20675.845
	3	0.08 < a/W < 0.15	1.0495253	-2.3396508	28.447540	-167.36188	524.24000	-674.54109
	4	0.15 < a/W < 0.35	0.99995068	-0.68716487	6.4143941	-20.474241	34.614535	-21.707134
	5	0.35 < a/W < 0.55	0.80303106	2.1259726	-9.6606769	25.454534	-30.998000	15.785743
	6	0.55 < a/W < 0.70	1.3337221	-2.6984910	7.8828269	-6.4427461	-2.0004730	5.2411878
	7	0.70 < a/W < 0.90	-108.19500	779.64954	-2227.3973	3186.8145	-2282.8985	656.92634

Table 3 – Coefficients αi of the piecewise polynomials of the reference geometry factor double-sided cracks in a long strip with an open hole

Single crack (Square plate with a hole)								
B/R	**Polynomial**	**Interval**	α_0	α_1	α_2	α_3	α_4	α_5
2	1	0 < a/W < 0.05	1.1199577	-0.78467247	9.0869927	-87.532458	798.28634	-3232.6665
	2	0.05 < a/W < 0.15	1.1189264	-0.68153317	4.9614206	-5.0210157	-26.828082	67.791201
	3	0.15 < a/W < 0.25	1.1274715	-0.96637028	8.7592487	-30.339870	57.568100	-44.737040
	4	0.25 < a/W < 0.45	1.0824820	-0.06658159	1.5609393	-1.5466322	-0.01837623	1.3321402
	5	0.45 < a/W < 0.65	0.96536456	1.2347237	-4.2226400	11.305766	-14.298819	7.6790035
	6	0.65 < a/W < 0.80	-17.005308	139.47067	-429.56401	665.67711	-517.66139	162.55979
	7	0.80 < a/W < 0.90	-1093.1349	6865.2808	-17244.089	21683.834	-13654.009	3446.6468
2.5	1	0 < a/W < 0.05	1.1200150	-1.1956259	11.1878891	-95.661546	765.95288	-2949.2844
	2	0.05 < a/W < 0.15	1.1190966	-1.1037842	7.5142215	-22.188194	31.219354	-10.350330
	3	0.15 < a/W < 0.25	1.1215821	-1.1866350	8.6188984	-29.552707	55.767732	-43.081500
	4	0.25 < a/W < 0.45	1.0786032	-0.32705612	1.7422674	-2.0461825	0.75468312	0.92893915
	5	0.45 < a/W < 0.65	0.95520483	1.0440368	-4.3514788	11.495476	-14.291604	7.6161777
	6	0.65 < a/W < 0.80	-15.647502	128.75717	-397.31495	616.05466	-479.33713	150.70711
	7	0.80 < a/W < 0.90	-1028.5758	6459.5592	-16224.320	20399.811	-12844.185	3241.9191
3	1	0 < a/W < 0.05	1.1200054	-1.5970855	14.115831	-117.17595	879.11469	-3275.4447
	2	0.05 < a/W < 0.15	1.1190040	-1.4969436	10.110154	-37.062415	77.979313	-70.903190
	3	0.15 < a/W < 0.25	1.1170745	-1.4326279	9.2526121	-31.345467	58.922819	-45.494530
	4	0.25 < a/W < 0.45	1.0718455	-0.52804671	2.0159623	-2.3988676	1.0296199	0.82002909
	5	0.45 < a/W < 0.65	0.95363220	0.78543414	-3.8217304	10.5737827	-13.384436	7.2262762
	6	0.65 < a/W < 0.80	-14.906594	122.78717	-379.21169	588.09679	-457.63291	143.91811
	7	0.80 < a/W < 0.90	-959.88892	6028.9267	-15144.561	19044.783	-11993.062	3027.7753
4	1	0 < a/W < 0.05	1.1201070	-2.4711928	26.421776	-280.64152	2290.6120	-8649.5021
	2	0.05 < a/W < 0.15	1.1174667	-2.2071598	15.860456	-69.415117	178.34794	-200.44593
	3	0.15 < a/W < 0.25	1.1060482	-1.8265456	10.785599	-35.582740	65.573352	-50.079808
	4	0.25 < a/W < 0.45	1.0574077	-0.8537345	3.0031107	-4.4527858	3.3134444	-0.2718814
	5	0.45 < a/W < 0.65	0.9192012	0.6818929	-3.8219000	10.713905	-13.538434	7.2178422
	6	0.65 < a/W < 0.80	-13.470834	111.37447	-344.41445	534.70244	-416.60654	131.23880
	7	0.80 < a/W < 0.90	-899.02533	5646.0901	-14181.203	17830.689	-11226.598	2833.7367
6	1	0 < a/W < 0.05	1.1201581	-4.1639508	57.853776	-710.20132	5961.4497	-22515.610
	2	0.05 < a/W < 0.15	1.1133119	-3.4793338	30.469096	-162.50772	484.51368	-607.86641
	3	0.15 < a/W < 0.25	1.0707548	-2.0607629	11.554818	-36.412534	64.196390	-47.443355
	4	0.25 < a/W < 0.45	1.0273729	-1.1931256	4.6137199	-8.6481394	8.6676019	-3.0203245
	5	0.45 < a/W < 0.65	0.81584227	1.1572151	-5.8322390	14.565102	-17.124889	8.4430048
	6	0.65 < a/W < 0.80	-11.290800	94.285229	-292.37997	455.40777	-356.23464	112.78447
	7	0.80 < a/W < 0.90	-836.80942	5253.7766	-13191.108	16578.818	-10433.366	2632.0674
6.27	1	0 < a/W < 0.05	1.1201718	-4.3953421	63.377169	-797.72436	6765.2945	-25641.557
	2	0.05 < a/W < 0.15	1.1123618	-3.6143459	32.137321	-172.92740	517.32500	-649.67859
	3	0.15 < a/W < 0.25	1.0669289	-2.0999138	11.944893	-38.311213	68.604358	-51.384407
	4	0.25 < a/W < 0.45	1.0187992	-1.1373209	4.2441500	-7.5082424	6.9984164	-2.0996541
	5	0.45 < a/W < 0.65	0.8449288	0.7945729	-4.3420449	11.572191	-14.202065	7.3227821
	6	0.65 < a/W < 0.80	-11.689475	97.213065	-301.01433	467.99109	-365.29353	115.35092
	7	0.80 < a/W < 0.90	-814.79973	5116.6521	-12849.612	16153.738	-10168.885	2566.2489
10	1	0 < a/W < 0.03	1.1199762	-7.3406837	144.48356	-2335.8682	27190.507	-155776.36
	2	0.03 < a/W < 0.08	1.1165298	-6.7662735	106.18954	-1059.4010	5916.0530	-13946.662
	3	0.08 < a/W < 0.15	1.0737770	-4.0942283	39.388415	-224.38687	697.21487	-899.56646
	4	0.15 < a/W < 0.35	1.0072763	-1.8775375	9.8325374	-27.347683	40.417589	-23.836744
	5	0.35 < a/W < 0.55	0.83643619	0.56303558	-4.1135945	12.498408	-16.505398	8.6906772
	6	0.55 < a/W < 0.70	1.1080975	-1.9066126	4.8669442	-3.8298445	-1.6615321	3.2929079
	7	0.70 < a/W < 0.90	-54.018535	391.85505	-1120.1664	1603.3606	-1149.6547	331.29096

Table 4 – Coefficients α_i of the piecewise polynomials of the reference geometry factor for a single crack in a square plate with an open hole

a/W	$\beta_1(a/W)$	$\beta_2(a/W)$	$\beta_3(a/W)$	$\beta_1(a/W)$	$\beta_2(a/W)$	$\beta_3(a/W)$
		B/R = 2			**B/R = 2.5**	
0.01	2.00000	1.28529	0.21898	2.00000	1.26170	0.21685
0.10	2.00000	1.16288	0.17866	2.00000	1.01491	0.16707
0.20	2.00000	1.32036	0.19725	2.00000	1.10098	0.18098
0.30	2.00000	1.64212	0.22673	2.00000	1.37595	0.19668
0.40	2.00000	2.11776	0.24249	2.00000	1.82218	0.18243
0.50	2.00000	2.77901	0.23364	2.00000	2.47546	0.11847
0.60	2.00000	3.74063	0.13090	2.00000	3.45661	-0.06981
0.70	2.00000	5.25440	-0.20008	2.00000	5.03195	-0.53088
0.80	2.00000	8.23762	-1.54974	2.00000	8.15079	-2.08486
0.90	2.00000	17.2563	-8.43988	2.00000	17.3699	-9.19363
		B/R = 3			**B/R = 4**	
0.01	2.00000	1.23832	0.21458	2.00000	1.19304	0.21007
0.10	2.00000	0.89890	0.16125	2.00000	0.72865	0.16008
0.20	2.00000	0.95035	0.18198	2.00000	0.75455	0.21793
0.30	2.00000	1.20611	0.20035	2.00000	1.00017	0.24764
0.40	2.00000	1.64092	0.17732	2.00000	1.43118	0.21394
0.50	2.00000	2.29478	0.08495	2.00000	2.08951	0.08901
0.60	2.00000	3.29032	-0.15090	2.00000	3.10796	-0.21048
0.70	2.00000	4.90532	-0.69152	2.00000	4.76603	-0.83892
0.80	2.00000	8.10360	-2.36561	2.00000	8.04881	-2.65058
0.90	2.00000	17.4535	-9.63238	2.00000	17.5907	-10.1651
		B/R = 6			**B/R = 10**	
0.01	2.00000	1.10970	0.20154	2.00000	0.97148	0.18887
0.10	2.00000	0.52456	0.19432	2.00000	0.32355	0.32754
0.20	2.00000	0.55447	0.31867	2.00000	0.40899	0.46707
0.30	2.00000	0.80961	0.35296	2.00000	0.68144	0.48155
0.40	2.00000	1.24595	0.29937	2.00000	1.14968	0.35622
0.50	2.00000	1.91705	0.12780	2.00000	1.82053	0.16775
0.60	2.00000	2.95930	-0.23811	2.00000	2.86196	-0.22943
0.70	2.00000	4.65592	-0.95080	2.00000	4.64309	-1.09906
0.80	2.00000	8.01591	-2.89337	2.00000	7.92295	-2.92529
0.90	2.00000	17.6317	-10.4884	2.00000	16.9183	-9.49277

Table 5 – $\beta_i(a/W)$ for double-sided cracks in a long strip with an open hole for B/R = 2, 2.5, 3, 4, 6, and 10

a/W	$\beta_1(a/W)$	$\beta_2(a/W)$	$\beta_3(a/W)$	$\beta_1(a/W)$	$\beta_2(a/W)$	$\beta_3(a/W)$
		B/R = 2			**B/R = 2.5**	
0.01	2.00000	1.28572	0.219049	2.00000	1.26141	0.216801
0.10	2.00000	1.17739	0.181897	2.00000	0.991449	0.173347
0.20	2.00000	1.32625	0.225686	2.00000	0.994673	0.205071
0.30	2.00000	1.57811	0.302179	2.00000	1.11937	0.245838
0.40	2.00000	1.90791	0.368565	2.00000	1.34242	0.251801
0.50	2.00000	2.34501	0.381964	2.00000	1.70234	0.170068
0.60	2.00000	3.00928	0.224581	2.00000	2.3337	-0.136998
0.70	2.00000	4.16543	-0.326358	2.00000	3.52733	-0.934857
0.80	2.00000	6.75977	-2.26821	2.00000	6.26417	-3.29225
0.90	2.00000	15.3653	-10.7821	2.00000	15.1545	-12.5816
		B/R = 3			**B/R = 4**	
0.01	2.00000	1.23758	0.21485	2.00000	1.18990	0.21034
0.10	2.00000	0.83385	0.16663	2.00000	0.57830	0.16307
0.20	2.00000	0.74325	0.19732	2.00000	0.38291	0.20682
0.30	2.00000	0.79849	0.22548	2.00000	0.37165	0.23810
0.40	2.00000	0.96762	0.20991	2.00000	0.49037	0.21744
0.50	2.00000	1.28808	0.09260	2.00000	0.77236	0.07893
0.60	2.00000	1.90080	-0.28031	2.00000	1.35939	-0.34390
0.70	2.00000	3.10859	-1.20195	2.00000	2.57018	-1.38563
0.80	2.00000	5.91244	-3.79448	2.00000	5.42401	-4.22927
0.90	2.00000	14.9072	-13.5079	2.00000	14.5182	-14.4791
		B/R = 6			**B/R = 6.27**	
0.01	2.00000	1.10042	0.20256	2.00000	1.08886	0.20153
0.10	2.00000	0.22189	0.18132	2.00000	0.18422	0.18496
0.20	2.00000	-0.05406	0.27571	2.00000	-0.09768	0.28787
0.30	2.00000	-0.10532	0.32795	2.00000	-0.14963	0.33961
0.40	2.00000	-0.01950	0.31555	2.00000	-0.06543	0.32842
0.50	2.00000	0.23757	0.16218	2.00000	0.18642	0.17934
0.60	2.00000	0.79458	-0.28629	2.00000	0.74374	-0.27717
0.70	2.00000	1.98850	-1.41514	2.00000	1.93787	-1.41564
0.80	2.00000	4.85832	-4.47437	2.00000	4.80027	-4.48068
0.90	2.00000	13.9435	-15.1551	2.00000	13.8811	-15.1951
		B/R = 10				
0.01	2.00000	0.94274	0.19086			
0.10	2.00000	-0.20590	0.27944			
0.20	2.00000	-0.50370	0.42868			
0.30	2.00000	-0.56920	0.50103			
0.40	2.00000	-0.47635	0.45528			
0.50	2.00000	-0.23818	0.30296			
0.60	2.00000	0.28826	-0.15400			
0.70	2.00000	1.50174	-1.40525			
0.80	2.00000	4.24168	-4.42383			
0.90	2.00000	12.5549	-14.2454			

Table 6 – $\beta_i(a/W)$ for a single crack in a square plate with an open hole for B/R = 2, 2.5, 3, 4, 6, 6.27 and 10

FIGURES

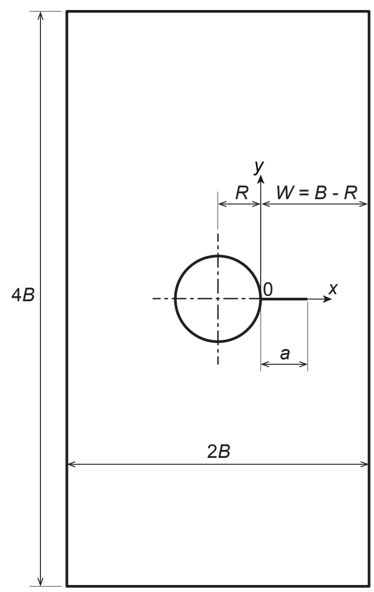

Figure 1 – Geometry of a finite width plate with a crack at a circular hole (after Wu and Carlsson [1])

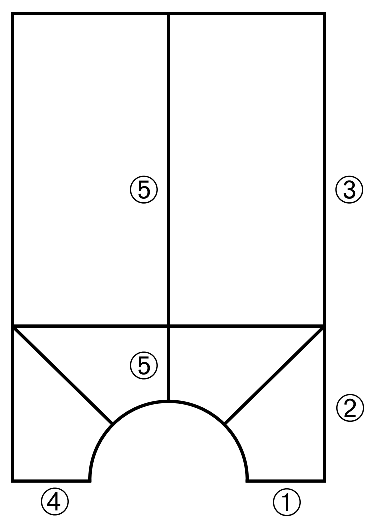

Figure 2 – Layout diagram for the two-dimensional FEM model of a half symmetric coupon (a simple depiction of the actual mesh would not be useful because node spacing is very small); features indicated by numeric labels (1) through (5) are described in the text

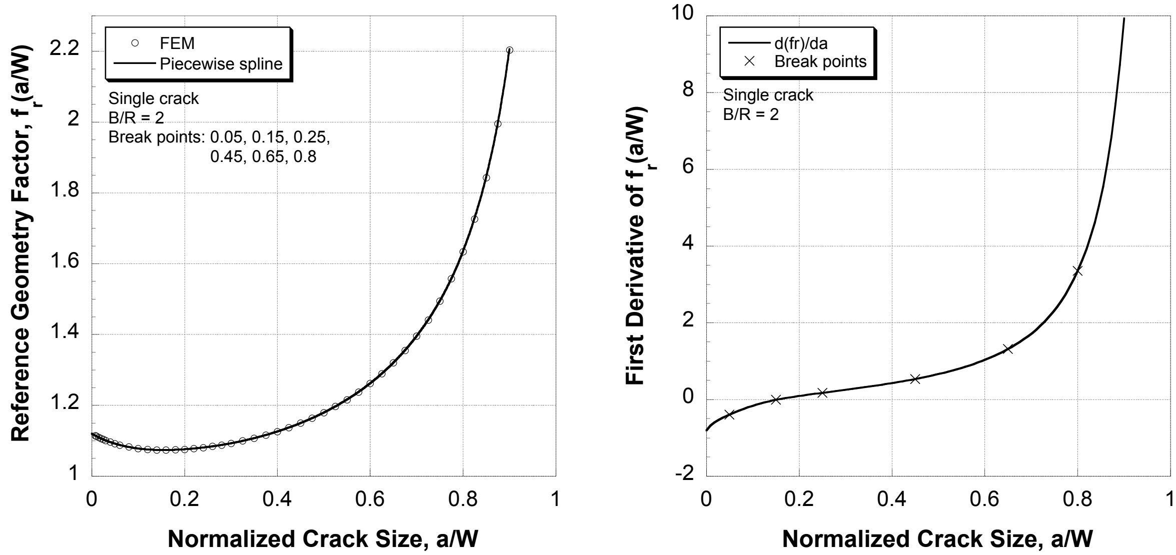

(a) *(b)*

Figure 3 – Piecewise spline fitting of the reference geometry factor resulting from FEM; (a) reference geometry factor fit, (b) the first derivative of the reference geometry factor fit

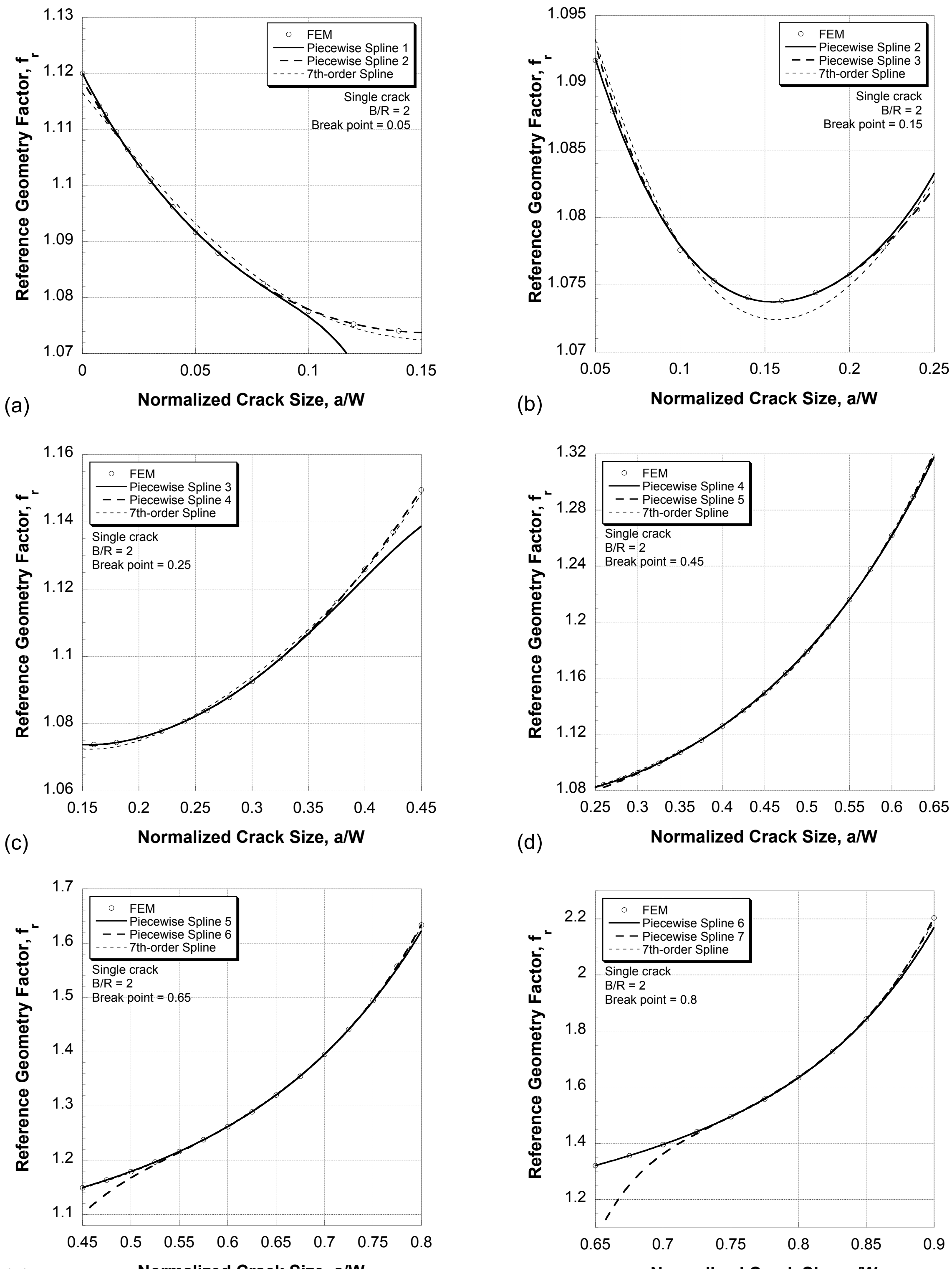

Figure 4 – 5^{th}-order piecewise spline fit and 7^{th}-order single spline fit of the reference geometry factors; splines for (a) $0 < a/W < 0.05$ and $0.05 < a/W < 0.15$, (b) $0.05 < a/W < 0.15$ and $0.15 < a/W < 0.25$, (c) $0.15 < a/W < 0.25$ and $0.25 < a/W < 0.45$, (d) $0.25 < a/W < 0.45$ and $0.45 < a/W < 0.65$, (e) $0.45 < a/W < 0.65$ and $0.65 < a/W < 0.8$, and (f) $0.65 < a/W < 0.8$ and $0.8 < a/W < 0.9$

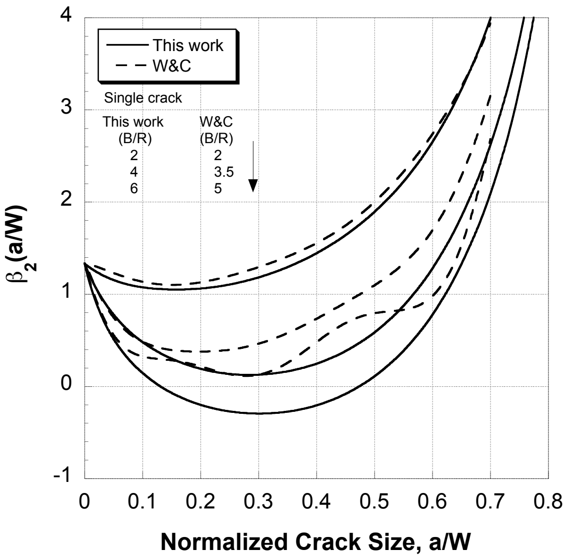

(a)

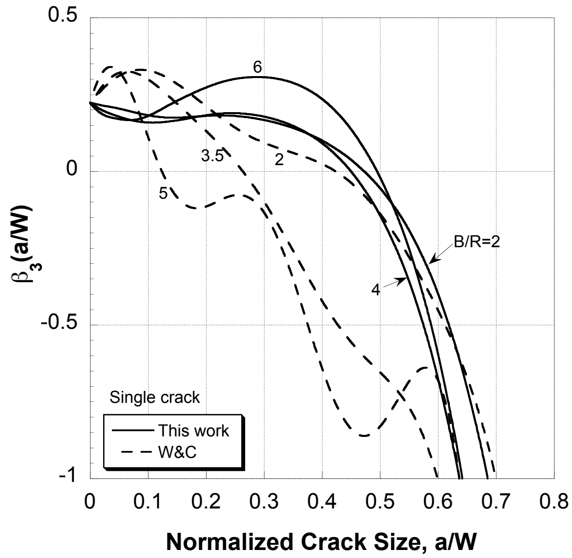

(b)

Figure 5 – (a) $\beta_2(a/W)$, and (b) $\beta_3(a/W)$ versus normalized crack size for B/R = 2, 4, and 6 for this work, and B/R = 2, 3.5, and 5 for Wu and Carlsson [1] (W&C)

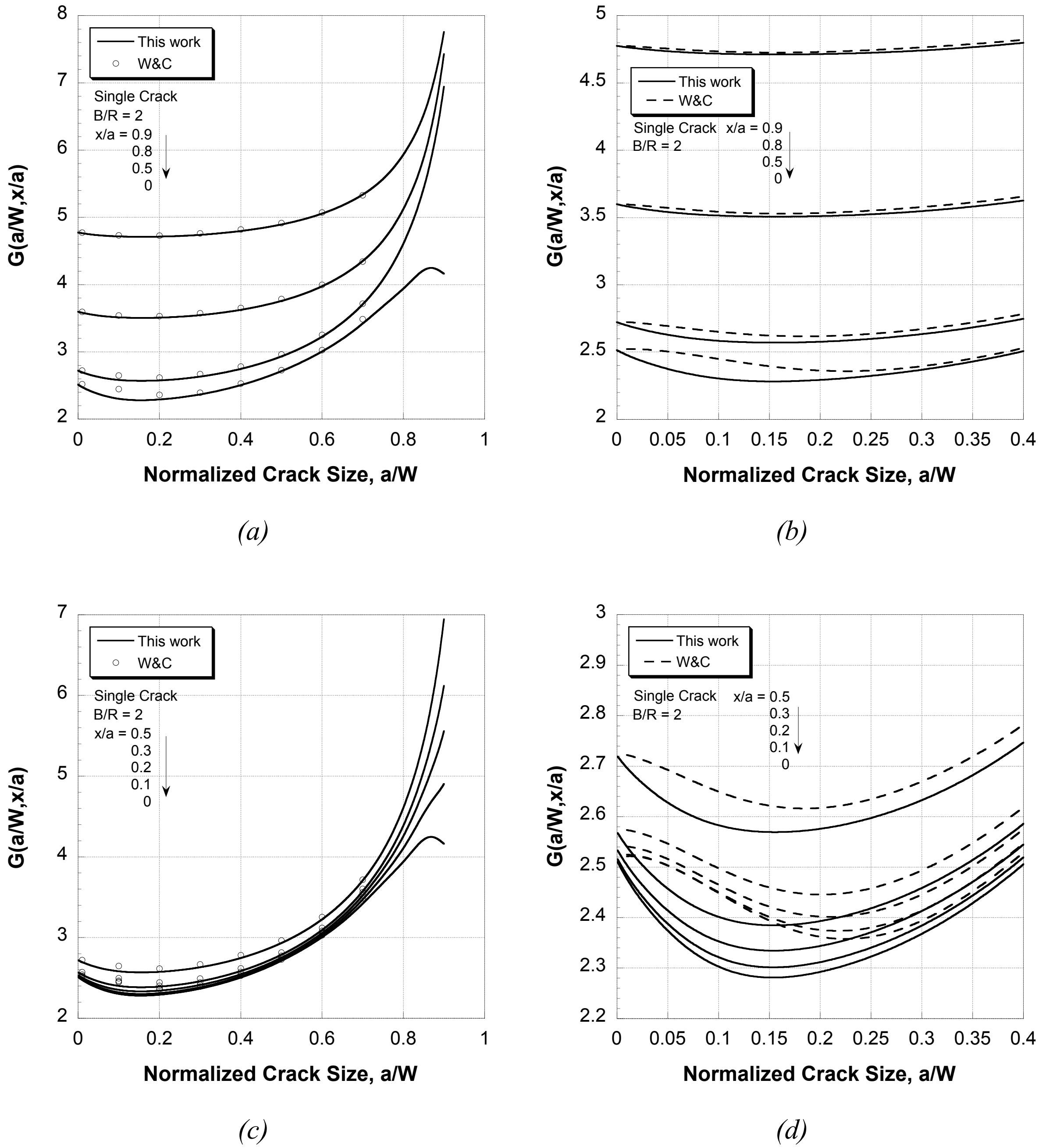

Figure 6 – Green's function results as a function of normalized crack size for point loads for a single crack in a long strip with an open hole (B/R = 2); (a) for the whole crack sizes at x/a = 0, 0.5, 0.8, and 0.9, (b) for 0 < a/W <0.4 at x/a = 0, 0.5, 0.8, and 0.9, (c) for the whole crack sizes at x/a = 0, 0.1, 0.2, 0.3, and 0.5, (d) for 0 < a/W <0.4 at x/a = 0, 0.1, 0.2, 0.3, and 0.5

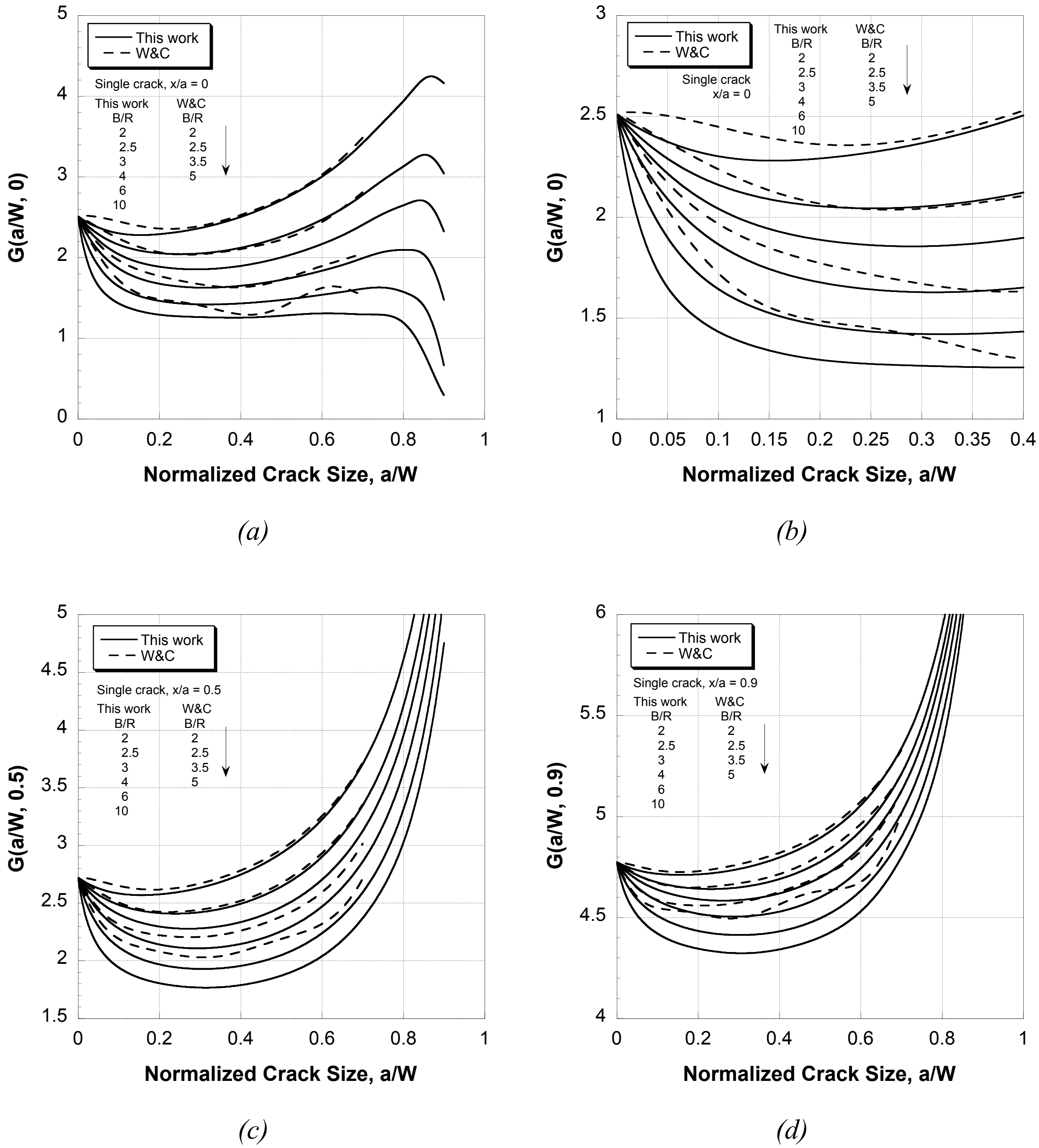

Figure 7 – Green's function results as a function of normalized crack size for point loads and various B/R ratios for a single crack in a long strip with an open hole; point load at (a) x/a = 0, (b) x/a = 0 for 0 < a/W <0.4, (c) x/a = 0.5, and (d) x/a = 0.9

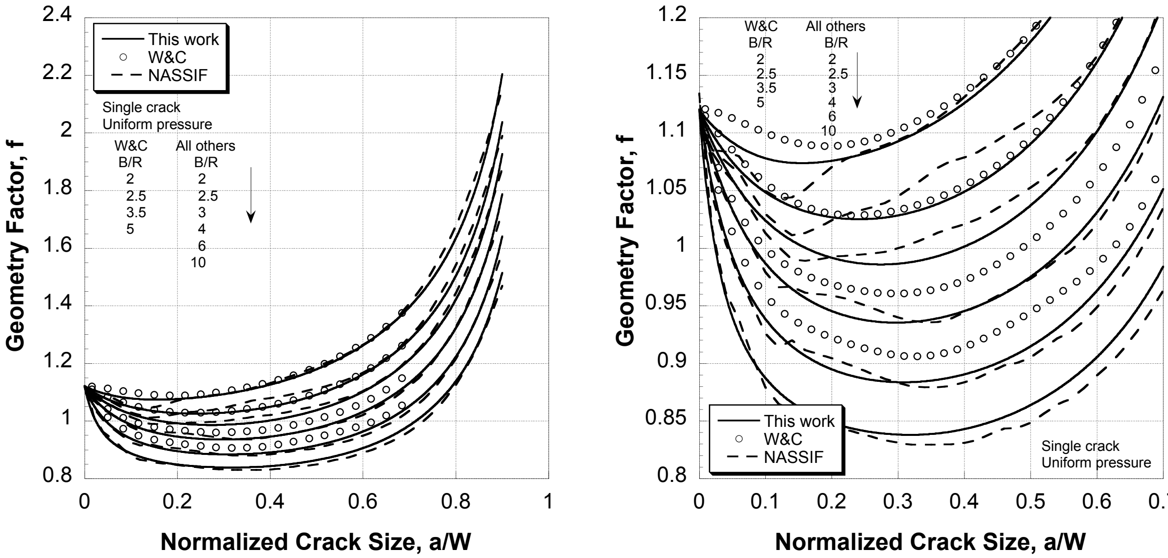

(a) (b)

Figure 8 – Geometry factor due to uniform crack-line pressure on a single crack as a function of normalized crack sizes for this work, W&C and NASSIF TC13 (NASGRO version 6.21); (a) for all a/W, and (b) for 0 < a/W < 0.6

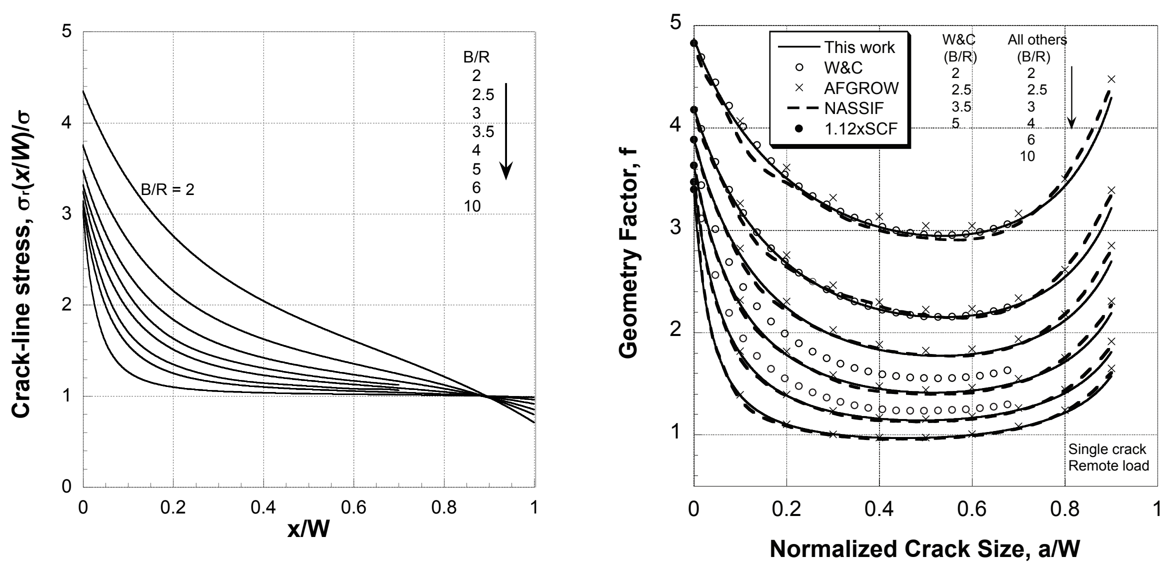

(a) (b)

Figure 9 – (a) Normalized crack-line stress due to remote load and (b) geometry factor as a function of normalized crack sizes for this work, W&C, AFGROW (version 4.0012.15), and NASSIF TC13 (NASGRO version 6.21)

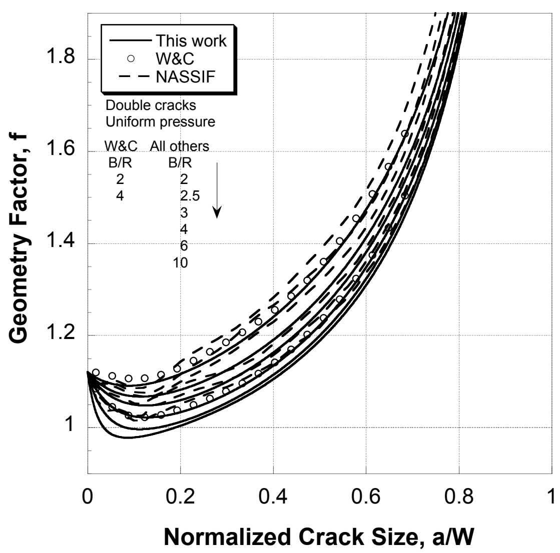

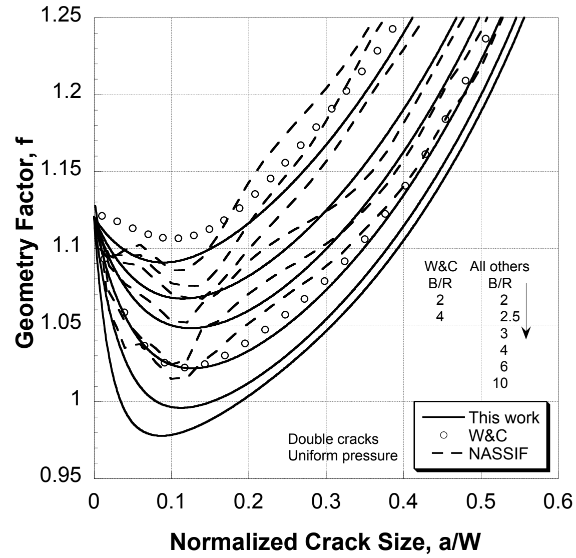

(a) *(b)*

Figure 10 – Geometry factor due to uniform crack-line pressure on double-sided cracks in a long strip with an open hole as a function of normalized crack sizes for this work, W&C and NASSIF; (a) for all a/W, and (b) for $0 < a/W < 0.6$

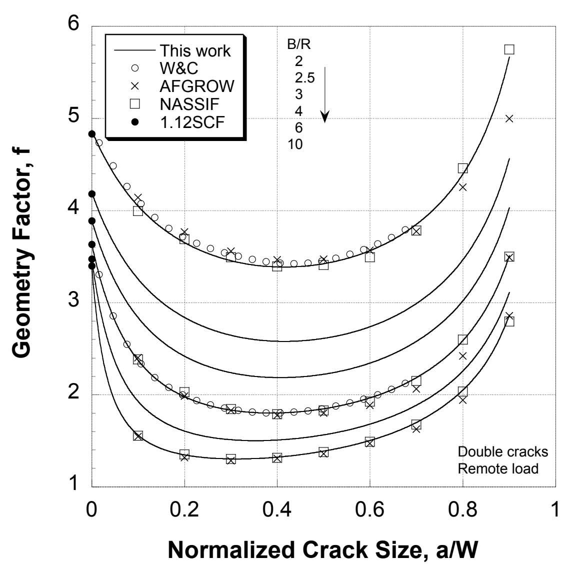

Figure 11 – Geometry factor due to remote load on double-sided cracks in a long strip with an open hole as a function of normalized crack sizes for this work, W&C, AFGROW (version 4.0012.15), and NASSIF (NASGRO version 6.21, solution TC13)

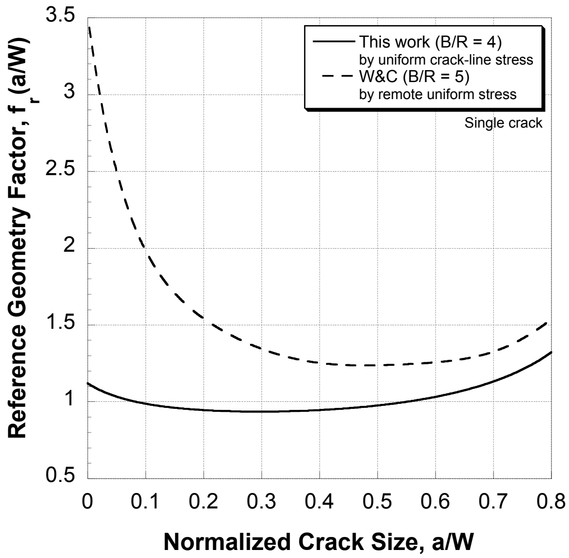

(a)

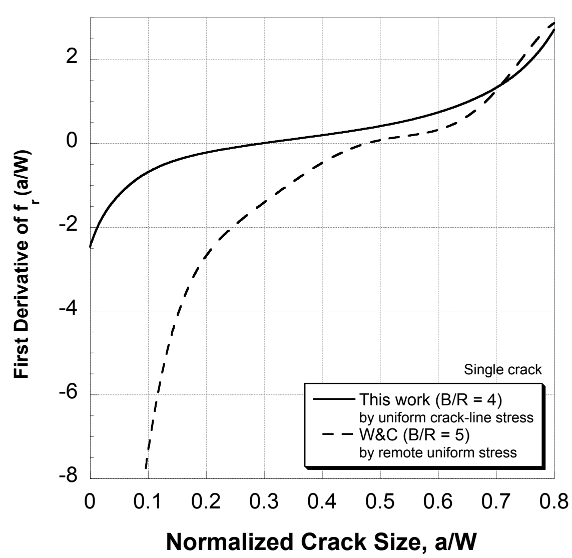

(b)

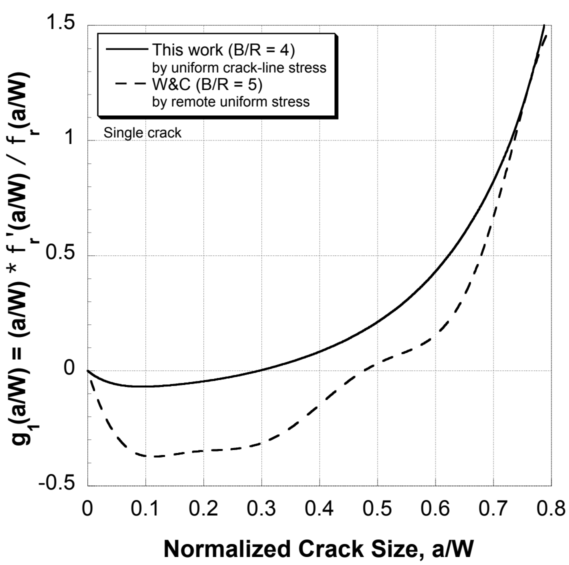

(c)

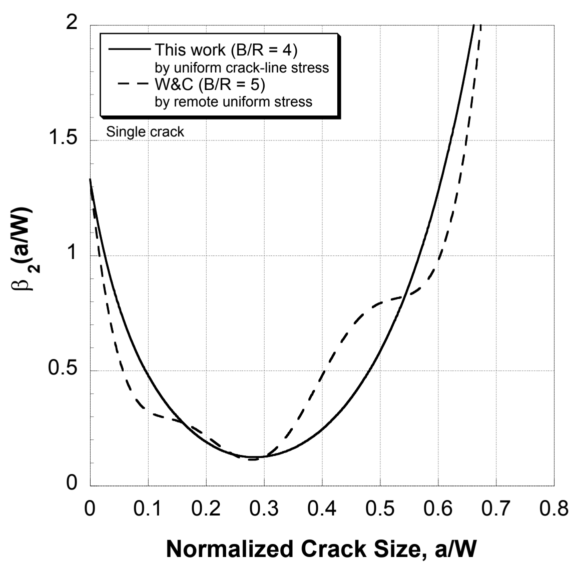

(d)

Figure 12 – Comparison of $\beta_2(a/W)$ and its major components for this work (B/R = 4) and W&C (B/R = 5) (LSN1); (a) Non-dimensional reference geometry factors, $f_r(a/W)$, (b) derivatives of the reference geometry factors, $f_r'(a/W)$, (c) $g_1(a/W)$, and (d) $\beta_2(a/W)$

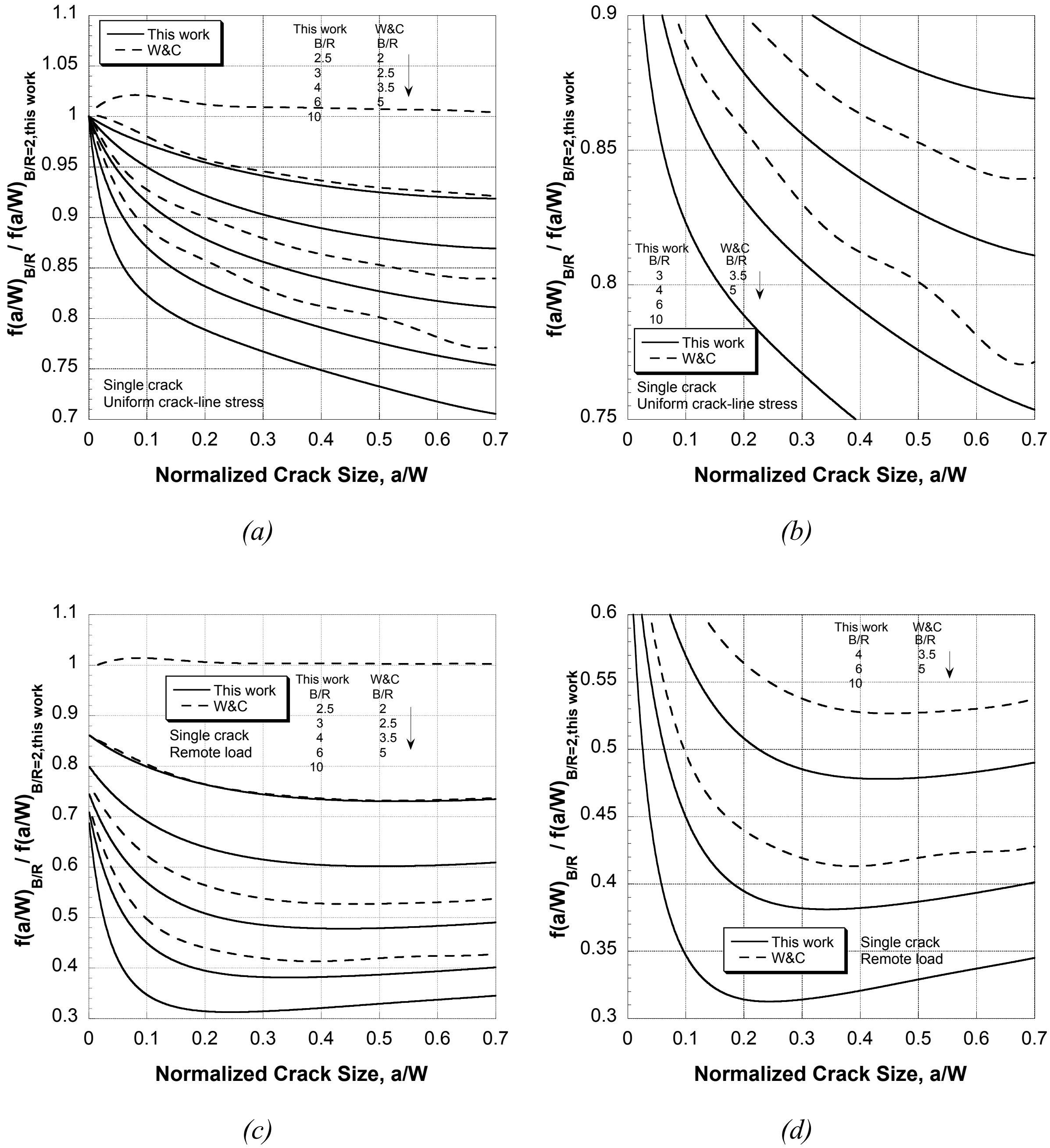

Figure 13 – Ratio of geometry factor for various B/R to geometry factor for B/R = 2 of this work, due to (a) unit uniform crack-line stress, (b) unit uniform crack-line stress magnified for vertical axis, (c) remote uniform stress, and (d) remote uniform stress magnified for vertical axis